ARTICLE

Light Generation and Harvesting in a van der Waals Heterostructure

Oriol Lopez-Sanchez,[†] Esther Alarcon Llado,[‡] Volodymyr Koman,[§] Anna Fontcuberta i Morral,[‡] Aleksandra Radenovic,[⊥] and Andras Kis[†,*]

[†]Electrical Engineering Institute, Ecole Polytechnique Federale de Lausanne (EPFL), CH-1015 Lausanne, Switzerland, [‡]Institute of Materials, Ecole Polytechnique Federale de Lausanne (EPFL), CH-1015 Lausanne, Switzerland, [§]Institute of Microtechnology, Ecole Polytechnique Federale de Lausanne (EPFL), CH-1015 Lausanne, Switzerland, and [⊥]Institute of Bioengineering, Ecole Polytechnique Federale de Lausanne (EPFL), CH-1015 Lausanne, Switzerland

ABSTRACT Two-dimensional (2D) materials are a new type of materials under intense study because of their interesting physical properties and wide range of potential applications from nanoelectronics to sensing and photonics. Monolayers of semiconducting transition metal dichalcogenides MoS_2 or WSe_2 have been proposed as promising channel materials for field-effect transistors. Their high mechanical flexibility, stability, and quality coupled with potentially inexpensive production methods offer potential advantages compared to organic and crystalline bulk semiconductors. Due to quantum mechanical confinement, the band gap in monolayer MoS_2 is direct in nature, leading to a strong interaction with light that can be exploited for building phototransistors and ultrasensitive photodetectors. Here, we report on the realization of light-emitting diodes based on vertical heterojunctions composed of n-type monolayer MoS_2 and p-type silicon. Careful interface engineering allows us to realize diodes showing rectification and light emission from the entire surface of the heterojunction. Electroluminescence spectra show clear signs of direct excitons related to the optical transitions between the conduction and valence bands. Our p—n diodes can also operate as solar cells, with typical external quantum efficiency exceeding 4%. Our work opens up the way to more sophisticated optoelectronic devices such as lasers and heterostructure solar cells based on hybrids of 2D semiconductors and silicon.

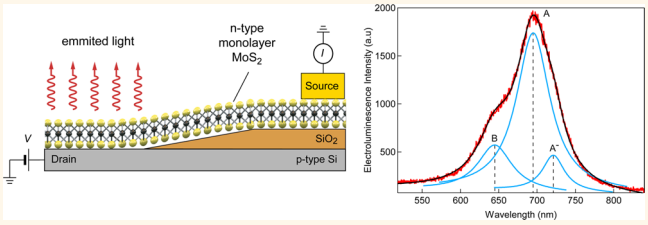

KEYWORDS: two-dimensional materials · dichalcogenides · MoS_2 · heterostructures · p—n junctions · nanophotonics · light-emitting diodes · solar cells

Molybdenum disulfide (MoS_2) is a typical representative of layered transition metal dichalcogenide (TMD) semiconductors[1] with electronic properties and a potential range of applications complementary to those of graphene. Bulk TMD crystals are stacks of layers held together *via* weak van der Waals interaction, allowing the extraction of single 2D atomic layers using the adhesive-type-based micromechanical cleavage technique[2] originally developed for the preparation of graphene. Because it has a band gap, monolayer MoS_2 can be used as the basic building block of room-temperature field-effect transistors[3] with an on/off ratio exceeding 10^8 as well as logic circuits[3] and amplifiers[4] with high gain. Large-area MoS_2 can also be grown using CVD-like growth techniques[5,6] or deposited using liquid phase exfoliation.[7−9]

The electronic and optical properties of monolayer MoS_2 and other semiconducting dichalcogenides are fundamentally different from those of their bulk counterparts. Because of the lack of inversion symmetry, charge carriers in monolayer MoS_2 behave as massive Dirac fermions,[10] while the conduction band of MoS_2 shows strong spin—orbit-induced spin splitting[11] and strong coupling of spin and valley degrees of freedom that can be detected using circularly polarized light[12−14] and could be used in novel devices based on the valley Hall effect.[15]

A transition from an indirect band gap to a direct band gap occurs in the monolayer limit,[16−19] manifesting itself in strong photoluminescence.[17,18] The direct band gap in MoS_2 can also be harnessed for the realization of vertical optoelectronic devices[20] as well as phototransistors[21] and photodetectors[22] with high responsivity and low noise-equivalent power.[22] Sundaram *et al.* recently demonstrated[23] that monolayer MoS_2 can also be used as a light emitter in an electroluminescent device with light

* Address correspondence to andras.kis@epfl.ch.

Received for review January 24, 2014 and accepted February 28, 2014.

Published online March 06, 2014
10.1021/nn500480u

emission occurring due to hot carrier processes in a region near locally gated contacts. While this result showed that monolayer MoS_2 could be used for the fabrication of light-emitting devices, the device geometry was limited by a relatively high power threshold for light emission and only a small portion of the device, restricted to the contact edge, was active in electroluminescence.

One way to overcome these factors limiting the exploitation of monolayer MoS_2 for practical applications in optoelectronic devices is to build light-emitting diodes based on vertical p−n junctions, resulting in a natural increase of the junction area that can easily be scaled. Reports on vertical p−n junctions based on TMD materials have been published before,[24] but these devices were not capable of electroluminescence and included thicker, indirect band gap TMD materials, which are less suitable for optoelectronic applications than their monolayer counterparts. We demonstrate here a vertical p−n junction in the form of a vertical heterostructure composed of n-type MoS_2 and p-type silicon serving as the hole injection layer.[25] We choose p-type silicon for this purpose because it is readily available and easy to pattern and handle. No reports on p-type monolayer MoS_2 have been published so far.

Our device shows a decreased threshold power for light emission, while the entire heterojunction surface is active as a light emitter. The device is also capable of operating as a solar cell.

RESULTS AND DISCUSSION

Figure 1 shows the structure of our device. Fabrication starts with exfoliation of MoS_2 (ref 2) onto an SiO_2/Si substrate. MoS_2 is then transferred[26] onto a prepatterned target highly doped p-type Si substrate[27] covered with SiO_2 with 1 μm × 1 to 100 μm × 100 μm windows through which the underlying Si is exposed. The native oxide on the substrate is removed and the Si surface passivated with hydrogen using a second wet etch step.[28]

In order to avoid degradation of the passivation layer, monolayer MoS_2 is immediately transferred across the edge of a window, exposing the Si surface (Figure 1a), and contacted on one side with a gold electrode. On the basis of AFM imaging we can see that MoS_2 is transferred on top of H−Si in a conformal fashion, with no visible voids or wrinkles. Both the 2D MoS_2 film and the H−Si substrate are terminated and have no dangling bonds at their surfaces, allowing the formation of a van der Waals heterostructure.[29] Because the nature of the interface is similar to that in graphene/BN heterostructures, we expect that most of the interface in our device is clean and free of contaminants,[30] allowing direct charge injection between Si and MoS_2. For diode characterization and electroluminescence measurements, we use the

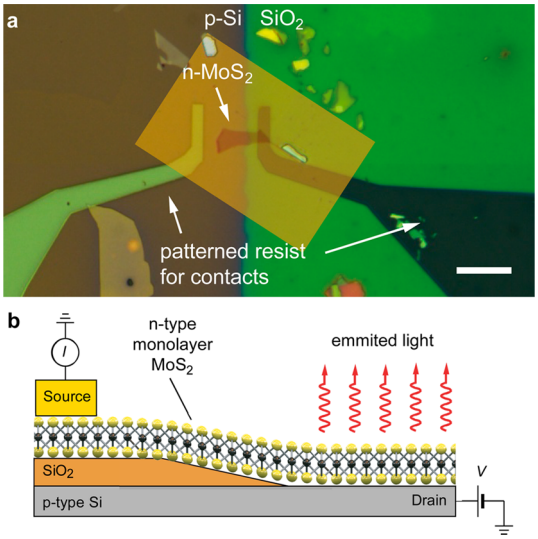

Figure 1. Geometry of the MoS_2/Si heterojunction light-emitting diode. (a) Optical image of the device in an intermediate state of fabrication. Monolayer MoS_2 is placed across the sidewall of a square window etched into a SiO_2 layer exposing the underlying p-doped silicon. Scale bar is 10 μm long. (b) Cross-sectional view of the structure of the device together with electrical connections used to induce light emission from the heterojunction. Electrons are injected from n-type MoS_2, while holes are injected from the p-Si substrate.

measurement scheme shown in Figure 1b. On some of the devices we also deposit a 30 nm thick HfO_2 or Al_2O_3 layer in order to encapsulate the device and increase the mobility in monolayer MoS_2.[31] This includes both devices presented here. More than 10 functioning devices were produced showing similar characteristics. We have observed that unencapsulated devices show a significant reduction of device currents and emitted light intensity when exposed to the ambient over the course of a week. The initial performance level can be restored by performing a vacuum anneal, indicating that the observed performance degradation could be due to adsorbed water and oxygen rather than an irreversible degradation of the interface. Encapsulated devices presented here show no significant change of performance over a period of at least one month.

Figure 2a shows the current *vs* bias voltage (I−V) characteristic of our MoS_2/Si heterojunction diode with 30 nm HfO_2 on top, exhibiting rectifying behavior with a current of 346 nA for a forward bias of 10 V and a junction area of 19 μm^2. This shows that classical diodes and all related optoelectronic devices could be prepared using a combination of an atomically thin 2D semiconductor and a 3D semiconductor, which should allow for a rapid fabrication and development of this type of device on industrial scales. We find that in the reverse bias regime a breakdown does not occur below −10 V.

In Figure 2b we outline the proposed band structure of our device, typical of type-II abrupt heterojunctions.[32] The junction is characterized by conduction

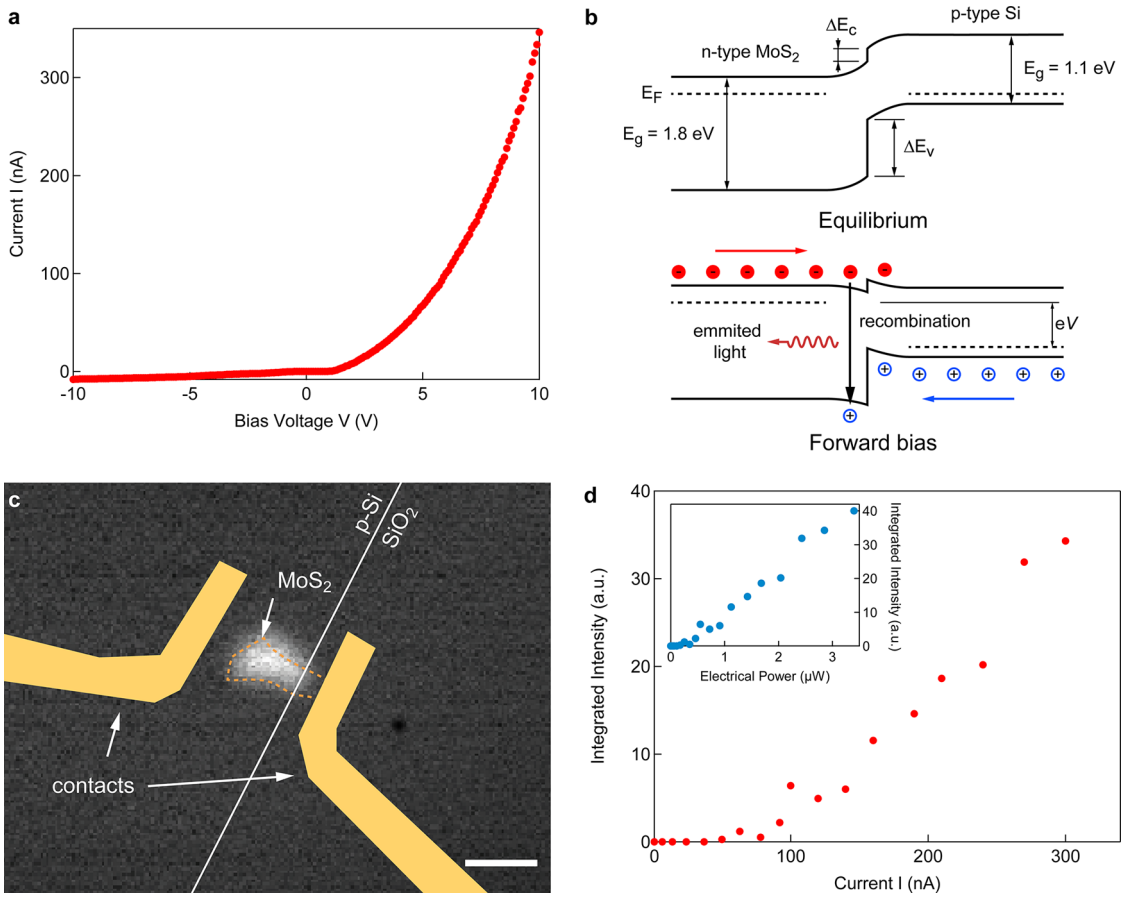

Figure 2. Electrical characteristic of the device. (a) Current *vs* bias voltage characteristic of the MoS_2/Si heterojunction diode. (b) Band diagram of the MoS_2/Si heterojunction in equilibrium conditions and under forward bias. Electrons injected from the n-MoS_2 and holes from p-Si can radiatively recombine in the junction. (c) Intensity map showing the electroluminescent emission with superimposed outline of the most important device components. The entire surface of the heterojunction is emitting light. Scale bar is 5 μm long. (d) Integrated light intensity as a function of device current. The inset shows the emitted light intensity as a function of electrical power. The threshold current for light emission is ~100 nA, corresponding to a threshold power of 3.2 W/cm^2 for a device with an active area of 19 μm^2.

(ΔE_C = 200 meV) and valence (ΔE_V = 900 meV) band offsets due to different electron affinities[33] and band gaps of Si and MoS_2. Under the application of forward bias V to the heterojunction, electrons injected from the MoS_2 side and holes injected from p-Si can radiatively recombine in the junction, resulting in light emission. Due to the direct band gap nature of MoS_2,[16−19] we expect the emitted light to be characterized by radiative transitions in MoS_2, as radiative transitions in Si are expected to be much less efficient due to its indirect band gap. Due to valence and conduction band offsets, discontinuities could occur in the bands with valence and conduction band cusps that can impair charge carrier injection efficiency and limit the device current.

The electroluminescent emission intensity map for a forward bias of 10 V is shown in Figure 2c, superposed on the outline of the device. Most of the heterojunction surface is active, in contrast to MoS_2 electroluminescent devices based on hot carrier processes in a region near locally gated contacts[23] or previously reported observations in a similar device geometry,[34] where the light emission was localized only at the heterojunction edge. The presence of a large active area in our device can be attributed to hydrogen passivation of the Si substrate, resulting in the formation of a true heterojunction with an efficient charge transfer. Large-area emitters such as the one presented here are also more attractive from a practical point of view because the total emitted light intensity could be more easily scaled up by simply increasing the device area.

Figure 2d shows the integrated electroluminescence intensity as a function of device current and electrical power for the active area centered on the heterojunction surface. The results show light emission from the device for bias voltages exceeding 5.5 V, corresponding to an electroluminescence threshold current of ~109 nA. The equivalent threshold power density is 3.2 W/cm^2, significantly lower than the previously reported threshold power of 15 kW/cm^2 for MoS_2 electroluminescent devices based on hot carrier injection.[23] This shows that the defect-free vertical heterojunction geometry and Si/MoS_2 band alignment are favorable for reducing the emission threshold and increasing the surface area of the emitter. The presence

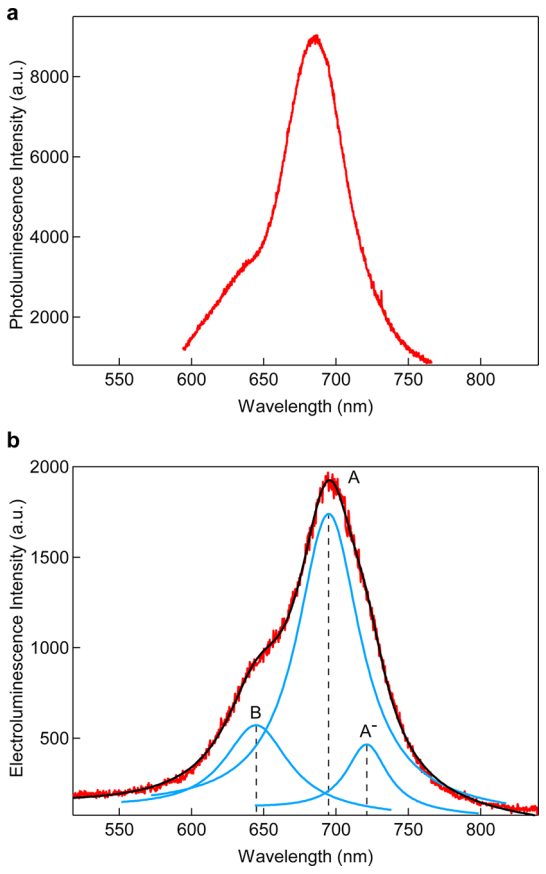

Figure 3. Light emission characteristics of the device. (a) Photoluminescence spectrum of the region of the monolayer MoS_2 flake supported by SiO_2. (b) Electroluminescence spectrum acquired under a forward bias $V = 15$ V and a current of 1.8 μA. The spectrum is fitted with three Lorentzian lines, which correspond to A and B excitons at 694 and 644 nm and the A^- trion resonance at 721 nm.

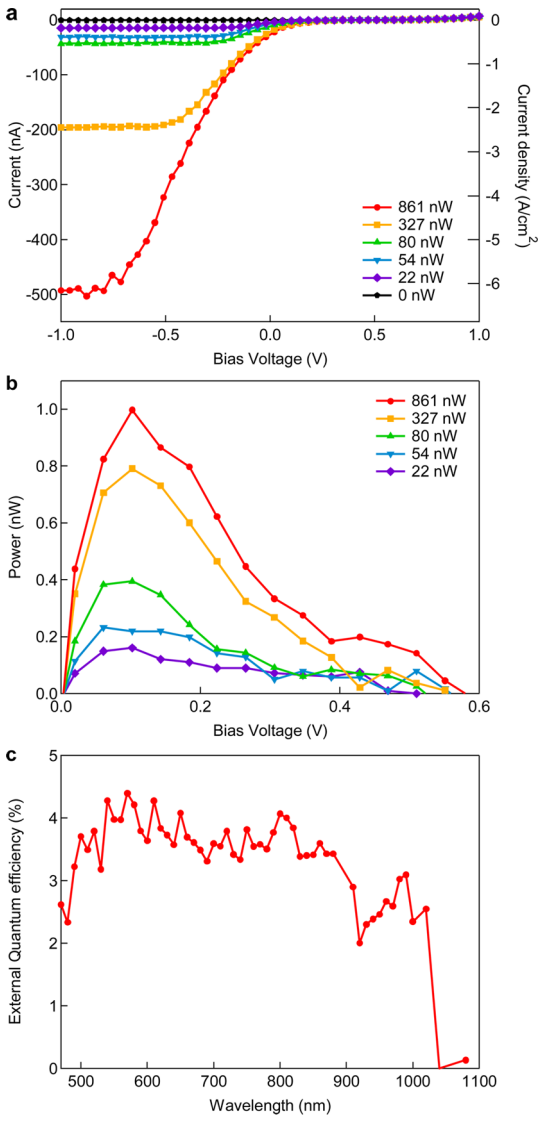

Figure 4. MoS_2/Si heterojunction as a solar cell. (a) Current as a function of bias voltage under different illumination powers from a 541 nm laser. The heterojunction area is 8 μm^2. (b) Electrical power generated by the device as a function of bias voltage, recorded for different illumination powers, extracted from data shown in a. (c) External quantum efficiency as a function of wavelength in the 450−1100 nm range for an illumination power of 500 nW. The curve shows a broadband response with MoS_2 and Si working in tandem and effectively extending the spectral response of MoS_2 into the infrared region. At both ends of the wavelength range, our measurements are limited by the sharp drop in emission intensity of our supercontinuum light source.

of a threshold is probably due to the existence of cusps in the heterojunction band diagram under forward bias conditions (Figure 2b) and could probably be further decreased with careful band engineering of the interface.

The photoluminescence (PL) spectrum of monolayer MoS_2 is acquired in the region where the flake is supported by SiO_2 and is shown in Figure 3a. The spectrum shows two peaks at 685 nm (1.81 eV) and 624 nm (1.98 eV). They are associated with excitonic transitions between the bottom of the conduction band and the top of the valence band, split due to spin−orbit coupling.[17,18,11]

In Figure 3b we show the electroluminescence spectrum, together with a fit to a multiple peak Lorentzian model. The main feature of the spectrum is a peak with a position of 694 nm (1.78 eV), which has a full width at half-maximum of 56 nm. The position of this peak matches well with the observed PL peak at 685 nm and is associated with the A exciton[12,17,18] in monolayer MoS_2. This shows that the relevant energy for the radiative recombination process in the MoS_2/Si heterojunction is the direct band gap in monolayer MoS_2. We observe an additional feature at 721 nm (1.72 eV), which can be related to the trion (negatively charged exciton) resonance in monolayer MoS_2.[35]

In addition to the A exciton, because of the low emission threshold, the electrical power density at which our device operates provides enough energy through impact ionization to excite the higher energy B exciton, which we can distinguish as an additional feature in the electroluminescence spectrum, located at 644 nm (1.92 eV). The small red shift with respect to

the related PL peak at 624 nm could be attributed to differences in the dielectric environments: the EL peak is acquired in the heterojunction region where MoS_2 is in direct contact with silicon, while the PL peak is acquired in the region where MoS_2 is supported by SiO_2. The difference in these two dielectric environments could affect the exciton binding energy through screening of the Coulomb interaction between electrons and holes.

The photoluminescence in the heterojunction area is strongly reduced in comparison to portions of the MoS_2 layer that are supported by SiO_2. This indicates the presence of an internal, open circuit voltage that separates the electrons and holes in the junction during the short period between light absorption and emission. This is favorable for operating our van der Waals heterostructures as solar cells. In Figure 4a we show current as a function of voltage in a second device with an area of 8 μm^2 for different illumination powers, showing the increase of short-circuit current under illumination, indicating power generation. The electrical power, P, generated in the device defined as $P = I \times V$ is shown in Figure 4b, with a peak power of ~1 nW for a bias voltage V = ~0.1 V and illumination power P_{inc} = 861 nW. We characterize the spectral response of the solar cell by measuring its short-circuit current, I_{sc} (obtained for a bias voltage of 0 V), as a function of illumination wavelength, λ, using a supercontinuum light source. The external quantum efficiency, EQE, of the device, defined as EQE = $(I_{sc}/P_{inc}) \times (hc/e\lambda)$, where h is Planck's constant, c the speed of light, and e the elementary charge, is shown in Figure 4c. It is characterized by a sharp drop above 1000 nm, coinciding with the absorption edge of silicon, and a broadband response in the 500–1000 nm region, indicating that MoS_2 and Si form a true p–n heterojunction instead of a Schottky contact and operate in tandem. The complementary absorption profiles of these materials result in a device with spectral response that is extended with respect to the response of monolayer MoS_2.[36] The maximum recorded EQE is 4.4%, which is a promising value for a device based on a two-dimensional monolayer and is more than an order of magnitude higher than in lateral p–n junctions based on the dichalcogenide WSe_2, which also shows a much narrower spectral response limited by its band gap.[37,38] The EQE could be further enhanced by careful control over doping levels of MoS_2 and Si, which would reduce the series resistance of the device, by use of large-area grown or deposited materials,[7,6,39] and by incorporating additional 2D semiconducting layers such as WSe_2 with complementary absorption spectra. Because of the direct band gap nature of monolayer MoS_2 and other dichalcogenide materials, we expect such future device cells to surpass the efficiencies of previously demonstrated solar cells based on bulk TMD semiconductors.[40]

CONCLUSION

To summarize, we show electroluminescent devices and solar cells based on heterojunctions composed of monolayer MoS_2 and p-type silicon. This choice of materials combines the advantages of the direct band gap and small thickness of 2D MoS_2 with the established silicon-based fabrication processes and could show the way to implementing 2D semiconductors as enabling materials in standard semiconductor fabrication lines. Furthermore, all the semiconducting materials used in our devices can be considered earth abundant and nontoxic. The entire junction area in our device participates in light emission with a low emission threshold power, allowing future large-area light emitters and lasers based on MoS_2. The low threshold power allows us to distinguish features in the emitted light spectra related to three different optical transitions, A and B excitons and the A^- trion resonance,[35] which could find valuable applications in the field of valleytronics. The heterojunction diode can also operate as a photovoltaic device, converting incoming light into electrical power with an external quantum efficiency of 4.4% and a broad spectral response, indicating that MoS_2 and silicon operate in tandem.

METHODS

Single layers of MoS_2 are exfoliated from commercially available crystals of molybdenite (SPI Supplies Brand Moly Disulfide) using the Scotch-tape micromechanical cleavage technique method pioneered for the production of graphene[41] on silicon substrates covered by a 270 nm layer of thermal oxide. Monolayer samples were identified by optical microscopy.[42] Once identified, monolayers were transferred[26] onto p-type silicon substrates with a resistivity of 0.1–0.5 Ωcm, corresponding to a boron doping level between 3×10^{16} and 3×10^{17} cm^{-3}, covered by a 100 nm thick layer of thermal SiO_2 with patterned holes from 1 $\mu m \times 1$ μm up to 100 $\mu m \times 100$ μm. Windows in SiO_2 are opened using 7:1 buffered oxide etch, resulting in sloped sidewalls. The initial etching step was followed by a 1 min 1% HF etch in order to remove the native oxide and passivate the Si surface.[28] The sample thickness was confirmed by photoluminescence measurements.

Monolayer MoS_2 diodes were characterized at room temperature. For electrical characterization, we use a gold electrode deposited on MoS_2 and a large-area electrode in direct contact with the p-Si substrate. A second gold electrode is deposited on top of Si near the MoS_2 flake but not in direct electrical contact with it. We use this electrode to verify that charge carriers can be injected from the passivated Si substrate. The emitted radiation was collected and analyzed using a grating spectrometer (HORIBA Jobin Yvon) equipped with a liquid nitrogen cooled CCD camera (Triax 550). An Andor iXon Ultra camera was used to perform photon counting and map the light emission. Photoluminescence measurements were performed using a laser centered at 488 nm and a spectrometer (Princeton Instruments SP-2500i) with a liquid nitrogen cooled camera (PiXIS/Pylon/Spec-10:256).

Heterojunction band structures were based on modeling performed using the Adept 2.0 tool available at NanoHUB.org.

Conflict of Interest: The authors declare no competing financial interest.

Acknowledgment. Device fabrication was carried out in part in the EPFL Center for Micro/Nanotechnology (CMI). Thanks go to Zdenek Benes for technical support with electron-beam lithography. We thank Olivier Martin (EPFL) for the use of the setup for the spectral characterization of electroluminescence as well as Jacopo Brivio and Simone Bertolazzi for technical help with the MoS_2 transfer. This work was financially supported by the Swiss Nanoscience Institute (NCCR Nanoscience). EAL and AFiM acknowledge funding through ERC Stg UpCon. AK acknowledges funding through ERC Stg FLATRONICS and AR through ERC Stg PorAbel.

REFERENCES AND NOTES

1. Wang, Q. H.; Kalantar-Zadeh, K.; Kis, A.; Coleman, J. N.; Strano, M. S. Electronics and Optoelectronics of Two-Dimensional Transition Metal Dichalcogenides. *Nat. Nanotechnol.* **2012**, *7*, 699–712.
2. Novoselov, K. S.; Jiang, D.; Schedin, F.; Booth, T. J.; Khotkevich, V. V.; Morozov, S. V.; Geim, A. K. Two-Dimensional Atomic Crystals. *Proc. Natl. Acad. Sci. U.S.A.* **2005**, *102*, 10451–10453.
3. Radisavljevic, B.; Whitwick, M. B.; Kis, A. Integrated Circuits and Logic Operations Based on Single-Layer MoS_2. *ACS Nano* **2011**, *5*, 9934–9938.
4. Radisavljevic, B.; Whitwick, M. B.; Kis, A. Small-Signal Amplifier Based on Single-Layer MoS_2. *Appl. Phys. Lett.* **2012**, *101*, 043103.
5. Liu, K.-K.; Zhang, W.; Lee, Y.-H.; Lin, Y.-C.; Chang, M.-T.; Su, C.-Y.; Chang, C.-S.; Li, H.; Shi, Y.; Zhang, H.; *et al.* Growth of Large-Area and Highly Crystalline MoS_2 Thin Layers on Insulating Substrates. *Nano Lett.* **2012**, *12*, 1538–1544.
6. Zhan, Y.; Liu, Z.; Najmaei, S.; Ajayan, P. M.; Lou, J. Large-Area Vapor-Phase Growth and Characterization of MoS_2 Atomic Layers on a Sio_2 Substrate. *Small* **2012**, *8*, 966–971.
7. Coleman, J. N.; Lotya, M.; O'Neill, A.; Bergin, S. D.; King, P. J.; Khan, U.; Young, K.; Gaucher, A.; De, S.; Smith, R. J.; *et al.* Two-Dimensional Nanosheets Produced by Liquid Exfoliation of Layered Materials. *Science* **2011**, *331*, 568–571.
8. Smith, R. J.; King, P. J.; Lotya, M.; Wirtz, C.; Khan, U.; De, S.; O'Neill, A.; Duesberg, G. S.; Grunlan, J. C.; Moriarty, G.; *et al.* Large-Scale Exfoliation of Inorganic Layered Compounds in Aqueous Surfactant Solutions. *Adv. Mater.* **2011**, *23*, 3944–3948.
9. Bertolazzi, S.; Brivio, J.; Kis, A. Stretching and Breaking of Ultrathin MoS_2. *ACS Nano* **2011**, *5*, 9703–9709.
10. Xiao, D.; Liu, G.-B.; Feng, W.; Xu, X.; Yao, W. Coupled Spin and Valley Physics in Monolayers of MoS_2 and Other Group-Vi Dichalcogenides. *Phys. Rev. Lett.* **2012**, *108*, 196802.
11. Zhu, Z. Y.; Cheng, Y. C.; Schwingenschlögl, U. Giant Spin-Orbit-Induced Spin Splitting in Two-Dimensional Transition-Metal Dichalcogenide Semiconductors. *Phys. Rev. B* **2011**, *84*, 153402.
12. Mak, K. F.; He, K.; Shan, J.; Heinz, T. F. Control of Valley Polarization in Monolayer MoS_2 by Optical Helicity. *Nat. Nanotechnol.* **2012**, *7*, 494–498.
13. Zeng, H.; Dai, J.; Yao, W.; Xiao, D.; Cui, X. Valley Polarization in MoS_2 Monolayers by Optical Pumping. *Nat Nanotechnol.* **2012**, *7*, 490–493.
14. Cao, T.; Wang, G.; Han, W.; Ye, H.; Zhu, C.; Shi, J.; Niu, Q.; Tan, P.; Wang, E.; Liu, B.; *et al.* Valley-Selective Circular Dichroism of Monolayer Molybdenum Disulphide. *Nat. Commun.* **2012**, *3*, 887–891.
15. Feng, W.; Yao, Y.; Zhu, W.; Zhou, J.; Yao, W.; Xiao, D. Intrinsic Spin Hall Effect in Monolayers of Group-Vi Dichalcogenides: A First-Principles Study. *Phys. Rev. B* **2012**, *86*, 165108.
16. Lebegue, S.; Eriksson, O. Electronic Structure of Two-Dimensional Crystals from ab Initio Theory. *Phys. Rev. B* **2009**, *79*, 115409.
17. Splendiani, A.; Sun, L.; Zhang, Y.; Li, T.; Kim, J.; Chim, C.-Y.; Galli, G.; Wang, F. Emerging Photoluminescence in Monolayer MoS_2. *Nano Lett.* **2010**, *10*, 1271–1275.
18. Mak, K. F.; Lee, C.; Hone, J.; Shan, J.; Heinz, T. F. Atomically Thin MoS_2: A New Direct-Gap Semiconductor. *Phys. Rev. Lett.* **2010**, *105*, 136805.
19. Kuc, A.; Zibouche, N.; Heine, T. Influence of Quantum Confinement on the Electronic Structure of the Transition Metal Sulfide Ts_2. *Phys. Rev. B* **2011**, *83*, 245213.
20. Britnell, L.; Ribeiro, R. M.; Eckmann, A.; Jalil, R.; Belle, B. D.; Mishchenko, A.; Kim, Y.-J.; Gorbachev, R. V.; Georgiou, T.; Morozov, S. V.; *et al.* Strong Light-Matter Interactions in Heterostructures of Atomically Thin Films. *Science* **2013**, *340*, 1311–1314.
21. Yin, Z.; Li, H.; Li, H.; Jiang, L.; Shi, Y.; Sun, Y.; Lu, G.; Zhang, Q.; Chen, X.; Zhang, H. Single-Layer MoS_2 Phototransistors. *ACS Nano* **2012**, *6*, 74–80.
22. Lopez-Sanchez, O.; Lembke, D.; Kayci, M.; Radenovic, A.; Kis, A. Ultrasensitive Photodetectors Based on Monolayer MoS_2. *Nat. Nanotechnol.* **2013**, *8*, 497–501.
23. Sundaram, R. S.; Engel, M.; Lombardo, A.; Krupke, R.; Ferrari, A. C.; Avouris, P.; Steiner, M., Electroluminescence in Single Layer MoS_2. *Nano Lett.* **2013**.
24. Späh, R.; Lux-Steiner, M.; Obergfell, M.; Bucher, E.; Wagner, S. N-$MoSe_2$/P-WSe_2 Heterojunctions. *Appl. Phys. Lett.* **1985**, *47*, 871–873.
25. Duan, X.; Huang, Y.; Agarwal, R.; Lieber, C. M. Single-Nanowire Electrically Driven Lasers. *Nature* **2003**, *421*, 241.
26. Brivio, J.; Alexander, D. T. L.; Kis, A. Ripples and Layers in Ultrathin MoS_2 Membranes. *Nano Lett.* **2011**, *11*, 5148–5153.
27. Yang, H.; Heo, J.; Park, S.; Song, H. J.; Seo, D. H.; Byun, K.-E.; Kim, P.; Yoo, I.; Chung, H.-J.; Kim, K. Graphene Barristor, a Triode Device with a Gate-Controlled Schottky Barrier. *Science* **2012**, *336*, 1140–1143.
28. Takahagi, T.; Nagai, I.; Ishitani, A.; Kuroda, H.; Nagasawa, Y. The Formation of Hydrogen Passivated Silicon Single-Crystal Surfaces Using Ultraviolet Cleaning and Hf Etching. *J. App. Phys.* **1988**, *64*, 3516–3521.
29. Koma, A. Van Der Waals Epitaxy - a New Epitaxial-Growth Method for a Highly Lattice-Mismatched System. *Thin Solid Films* **1992**, *216*, 72–76.
30. Haigh, S. J.; Gholinia, A.; Jalil, R.; Romani, S.; Britnell, L.; Elias, D. C.; Novoselov, K. S.; Ponomarenko, L. A.; Geim, A. K.; Gorbachev, R. Cross-Sectional Imaging of Individual Layers and Buried Interfaces of Graphene-Based Heterostructures and Superlattices. *Nat. Mater.* **2012**, *11*, 764–767.
31. Radisavljevic, B.; Kis, A. Mobility Engineering and a Metal-Insulator Transition in Monolayer MoS_2. *Nat. Mater.* **2013**, *12*, 815–820.
32. Kroemer, H. Heterostructure Bipolar Transistors and Integrated Circuits. *Proc. IEEE* **1982**, *70*, 13–25.
33. Kang, J.; Tongay, S.; Zhou, J.; Li, J.; Wu, J. Band Offsets and Heterostructures of Two-Dimensional Semiconductors. *Appl. Phys. Lett.* **2013**, *102*, 012111.
34. Ye, Y.; Ye, Z.; Gharghi, M.; Zhu, H.; Zhao, M.; Yin, X.; Zhang, X. Exciton-Related Electroluminescence from Monolayer MoS_2. *arXiv.org, e-Print Arch., Condens. Matter* **2013**, 1305.4235.
35. Mak, K. F.; He, K.; Lee, C.; Lee, G. H.; Hone, J.; Heinz, T. F.; Shan, J. Tightly Bound Trions in Monolayer MoS_2. *Nat. Mater.* **2013**, *12*, 207–211.
36. Bernardi, M.; Palummo, M.; Grossman, J. C. Extraordinary Sunlight Absorption and One Nanometer Thick Photovoltaics Using Two-Dimensional Monolayer Materials. *Nano Lett.* **2013**, *13*, 3664–3670.
37. Pospischil, A.; Furchi, M. M.; Mueller, T. Solar Energy Conversion and Light Emission in an Atomic Monolayer p-n Diode. *arXiv.org e-Print Arch., Condens. Matter* **2013**, 1309.7492.
38. Baugher, B. W. H.; Churchill, H. O. H.; Yafang, Y.; Jarillo-Herrero, P. Electrically Tunable Pn Diodes in a Monolayer Dichalcogenide. *arXiv.org e-Print Arch., Condens. Matter* **2013**, 1310.0452.

39. Liu, K.-K.; Zhang, W.; Lee, Y.-H.; Lin, Y.-C.; Chang, M.-T.; Su, C.-Y.; Chang, C.-S.; Li, H.; Shi, Y.; Zhang, H.; *et al*. Growth of Large-Area and Highly Crystalline MoS_2 Thin Layers on Insulating Substrates. *Nano Lett.* **2012**, *12*, 1538–1544.
40. Tenne, R.; Wold, A. Passivation of Recombination Centers in N-WSe_2 Yields High Efficiency (>14%) Photoelectrochemical Cell. *Appl. Phys. Lett.* **1985**, *47*, 707.
41. Novoselov, K. S.; Geim, A. K.; Morozov, S. V.; Jiang, D.; Zhang, Y.; Dubonos, S. V.; Grigorieva, I. V.; Firsov, A. A. Electric Field Effect in Atomically Thin Carbon Films. *Science* **2004**, *306*, 666–669.
42. Benameur, M. M.; Radisavljevic, B.; Heron, J. S.; Sahoo, S.; Berger, H.; Kis, A. Visibility of Dichalcogenide Nanolayers. *Nanotechnology* **2011**, *22*, 125706.